

Supporting Information for

Effect of commensurate Lithium doping on the scintillation of two-dimensional perovskite crystals.

Francesco Maddalena^{1,2,*}, *Aozhen Xie*^{1,2}, *Arramel Arramel*, *Marcin E. Witkowski*⁴, *Michal Makowski*⁴, *Benoit Mahler*⁵, *Winicjusz Drozdowski*⁴, *Thambidurai Mariyappan*^a, *Stuart Victor Springham*⁶, *Philippe Coquet*^{1,2,7}, *Christophe Dujardin*⁵, *Muhammad Danang Birowosuto*^{1,2,*}, and *Cuong Dang*^{1,2,*}

¹School of Electrical and Electronic Engineering, Nanyang Technological University, 50 Nanyang Avenue, 639798, Singapore

²CINTRA UMI CNRS/NTU/THALES 3288, Research Techno Plaza, 50 Nanyang Drive, Border X Block, Level 6, 637553, Singapore

³Department of Physics, National University of Singapore, 2 Science Drive 3, 117542 Singapore, Singapore.

⁴Institute of Physics, Faculty of Physics, Astronomy, and Informatics, Nicolaus Copernicus University in Torun, ul. Grudziadzka 5, 87-100 Torun, Poland

⁵Université de Lyon, Université Claude Bernard, Lyon 1, CNRS, Institut Lumière Matière UMR5306, Villeurbanne F-69622, France

⁶Natural Sciences and Science Education, National Institute of Education, 1 Nanyang Walk, 637616, Singapore

⁷Institute of Electronics, Microelectronics and Nanotechnologies (IEMN), CNRS UMR 8520-University of Lille, 59650 Villeneuve d'Ascq Cedex, France

*Corresponding Authors.

Email: francesco_maddalena@ntu.edu.sg; mbirowosuto@ntu.edu.sg; hcdang@ntu.edu.sg

Sheet List

Supplementary Figure S1. XRD diffractograms for the investigated perovskites and the respective theoretical lines.

Supplementary Table S1. Li doping levels measured from XPS and ICPMS.

Supplementary Figure S2. Temperature-dependent RL spectra for the undoped and Li-doped $\text{PEA}_2\text{PbBr}_4$ and BA_2PbBr_4 .

Supplementary Figure S3. Fluorescence spectra for $\text{PEA}_2\text{PbBr}_4$ and BA_2PbBr_4 .

Supplementary Table S2. FWHM values of the RL peak at room temperature for the investigated perovskites.

Supplementary Figure S4. Microcapillary plate template.

Supplementary Table S3. Fitting parameters of the negative thermal quenching of the radioluminescence.

Supplementary Table S4. Residual radioluminescence and fit parameters of the afterglow decay at 10 K.

Supplementary Figure S5. Thermoluminescence peaks for Li-doped $\text{PEA}_2\text{PbBr}_4$ (left) and BA_2PbBr_4 (right) and the corresponding fits.

Supplementary Table S5. Parameters of the thermoluminescence peak fitting.

Supplementary Figure S6. Current-voltage curves for undoped and Li-doped $\text{PEA}_2\text{PbBr}_4$ (left) and BA_2PbBr_4 (right) measured in darkness and under white light.

Supplementary Figure S7. Fitting of a decay curves for radiation hardness and normalized decay times.

Supplementary Table S6. Decay times of the room temperature RL under constant X-ray irradiation.

Supplementary Figure S8. Photoluminescence intensity vs. time of the investigated perovskites while exposed to environmental conditions (standard atmosphere, 65 % humidity).

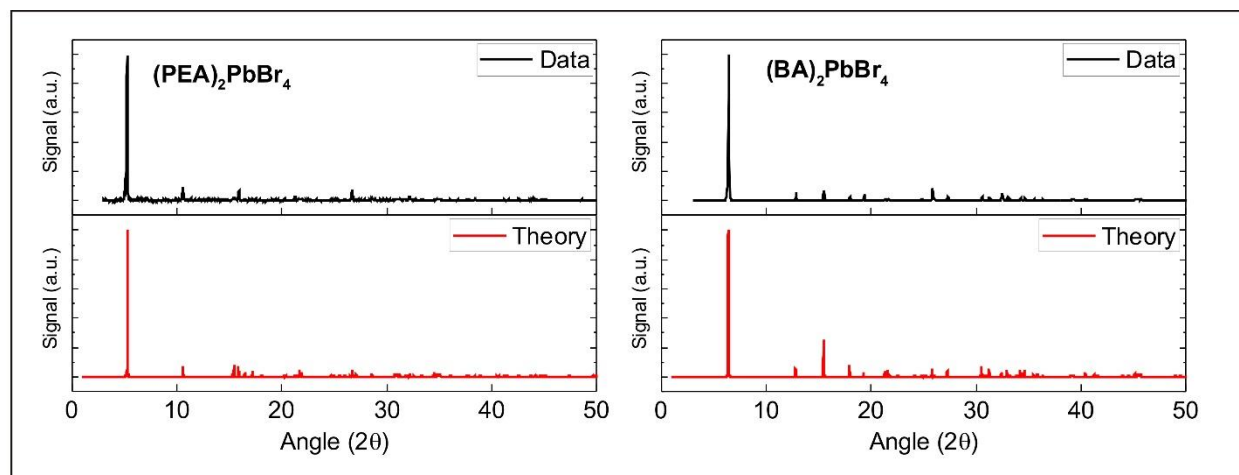
Supplementary Figure S9. Peak values of the normalized RL of the undoped and Li-doped perovskites at room temperature at different voltage and current applies to the X-ray source.

Supplementary Table S7. Normalized light yield for the undoped and Li-doped perovskites at different gamma-ray excitation energies.

Supplementary Table S8. Energy resolution of the undoped and Li-doped perovskites at different gamma-ray excitation energies.

Supplementary Table S9. Fitting parameters for the scintillation decay of the investigated perovskites under gamma-ray excitation ($E = 662$ keV) at room temperature.

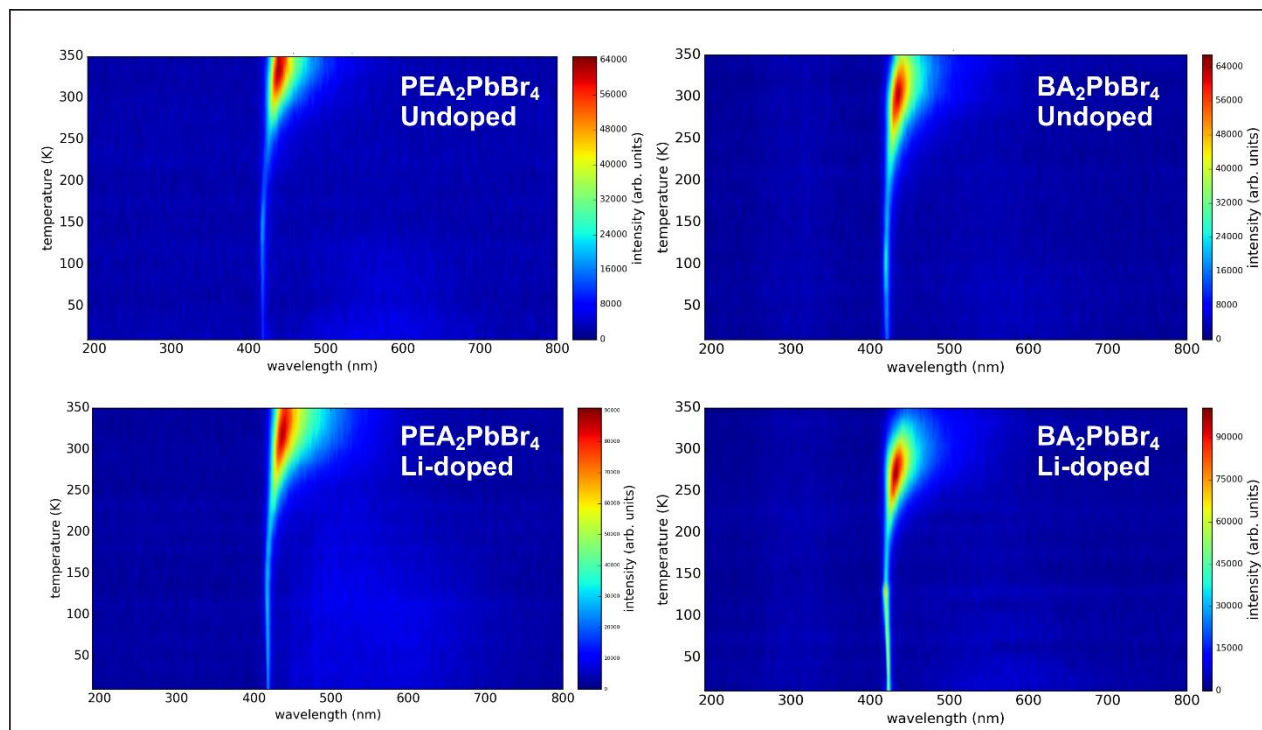
Supplementary Figure S10. The X-ray luminescence intensity of undoped (left) and Li-doped (right) octylammonium lead bromide.



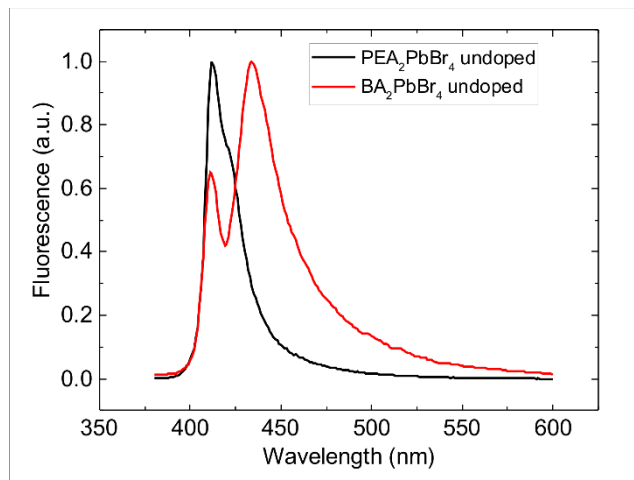
Supplementary Figure S1. Measured XRD diffractograms for $\text{PEA}_2\text{PbBr}_4$ and BA_2PbBr_4 and the respective theoretical diffractograms.

Supplementary Table S1. Li doping amounts obtained by XPS and ICPMS measurements.

Sample	Li doping (% of Pb-atoms)	
	XPS	ICPMS
Undoped $\text{PEA}_2\text{PbBr}_4$	0	0
Li-doped $\text{PEA}_2\text{PbBr}_4$	5.4	4.4
Undoped BA_2PbBr_4	0	0
Li-doped BA_2PbBr_4	3.7	3.8



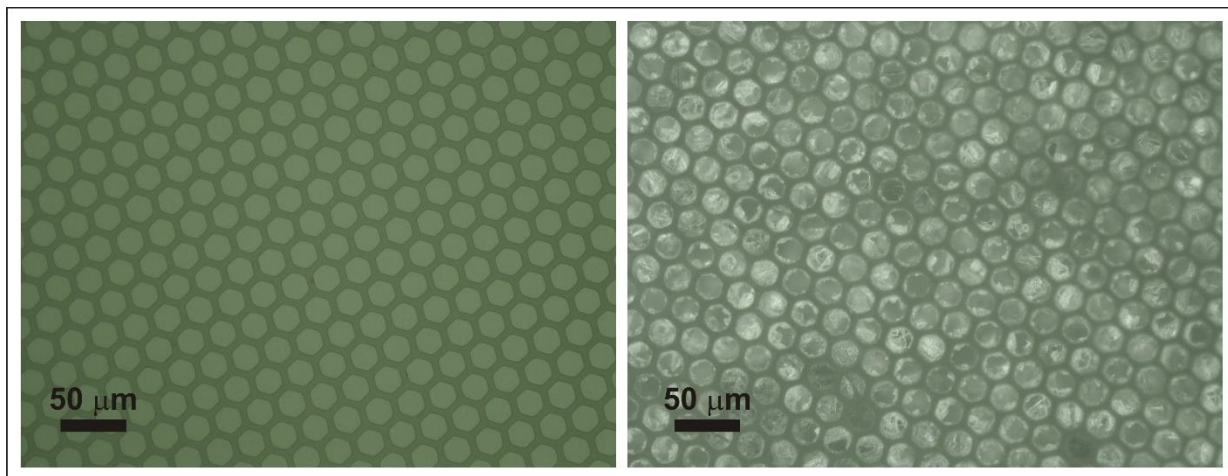
Supplementary Figure S2. Temperature-dependent RL spectra for the undoped and Li-doped PEA₂PbBr₄ and BA₂PbBr₄.



Supplementary Figure S3. Fluorescence spectra for $\text{PEA}_2\text{PbBr}_4$ and BA_2PbBr_4 .

Supplementary Table S2. FWHM values for the RL peaks at room temperature of the investigated perovskites.

Sample	FWHM (nm)
$\text{PEA}_2\text{PbBr}_4$	30
$\text{PEA}_2\text{PbBr}_4$ Li-doped	41
BA_2PbBr_4	27
BA_2PbBr_4 Li-doped	35



Supplementary Figure S4. Dark-field image of the pristine (left) and perovskite-filled (right) microcapillary template.

Negative thermal quenching behavior analysis

For our analysis, we apply the simplest case of the analytical model derived by Shibata(1998)¹:

$$\|I(T)\| = \frac{1+D \cdot \exp(-E_1'/k_B T)}{1+C \cdot \exp(-E_1/k_B T)} \quad (\text{SE1})$$

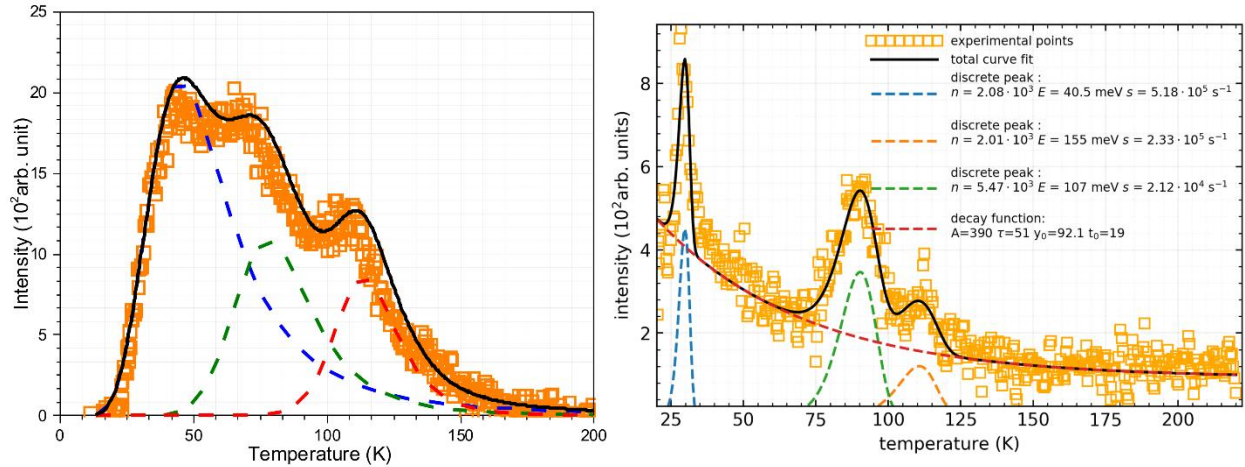
where $\|I(T)\|$ is the integrated radioluminescence emission intensity at absolute temperature T normalized to the maximum integrated intensity, D is the negative thermal quenching coefficient which describes the contribution from thermally excited electrons, C is the thermal quenching coefficient related to non-radiative electron excitation, E_1' and E_1 are the activation energies for negative thermal quenching and typical thermal quenching and k_B is the Boltzmann constant. The fitting parameters are listed in Supplementary Table 2, below.

Supplementary Table S3. Fitting parameters of negative thermal quenching of the radioluminescence using Equation SE1.

Sample	D	C	E_1' (meV)	E_1 (meV)
Undoped PEA ₂ PbBr ₄	6.69×10^5	2.46×10^5	4.38	4.30
Li-doped PEA ₂ PbBr ₄	3.01×10^6	5.93×10^6	4.87	4.87
Undoped BA ₂ PbBr ₄	4.96×10^5	1.03×10^6	4.07	4.03
Li-doped BA ₂ PbBr ₄	7.09×10^5	1.43×10^6	5.20	5.08

Supplementary Table S4. Residual radioluminescence after 5 s at 10 K and fit parameters of the afterglow decay at 10 K, fitted with a multiple exponential decay, where τ_i is the decay time, C_i is the contribution of the decay time and $\bar{\tau}$ is the mean time of the decay. The decay of undoped BA_2PbBr_4 was too fast to be fitted accurately.

Sample	Residual RL after 5s (%)	Afterglow Decay parameters τ_i (s) / C_i (%)	Afterglow Average Decay Time $\bar{\tau}$ (s)
Undoped $\text{PEA}_2\text{PbBr}_4$	< 1	10.3 / 83.3 82.2 / 16.7	22.3
Li-doped $\text{PEA}_2\text{PbBr}_4$	1.7	16.3 / 61.1 157.6 / 38.9	71.3
Undoped BA_2PbBr_4	< 1	n/a	n/a
Li-doped BA_2PbBr_4	2.1	17.1 / 80.4 352.1 / 19.6	82.8

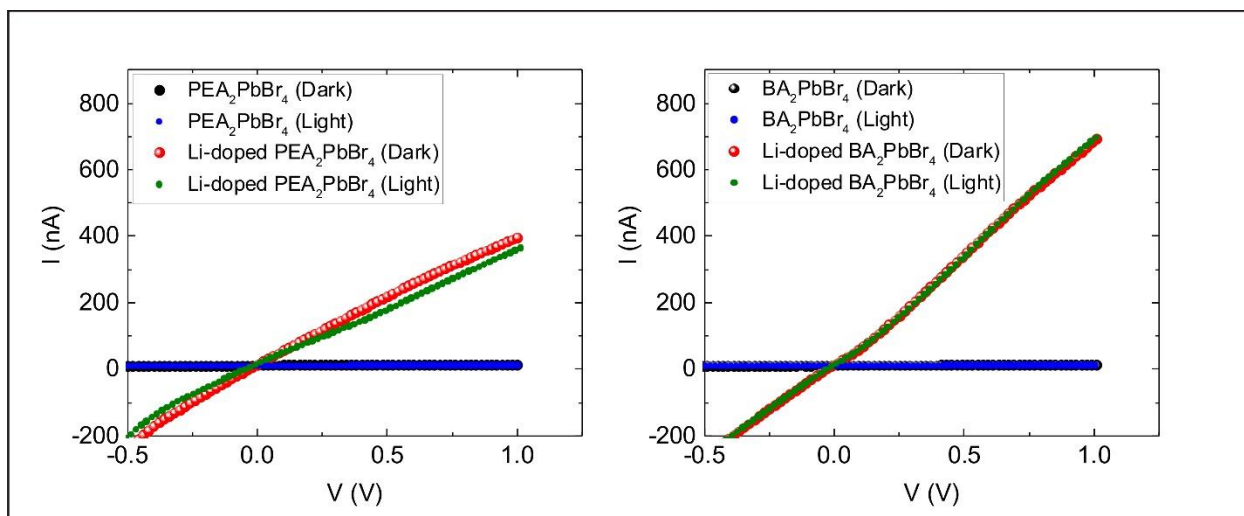


Supplementary Figure S5. Thermoluminescence peaks for Li-doped $\text{PEA}_2\text{PbBr}_4$ (left) and BA_2PbBr_4 (right) and the corresponding fits.

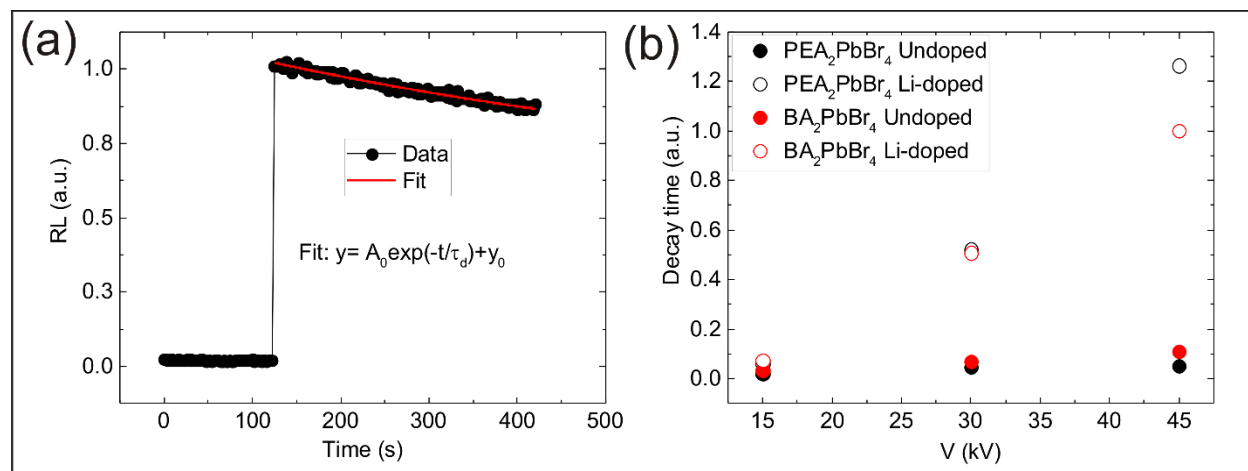
Fitting of the thermoluminescence glow peaks. We start with the assumption that the traps in the thermoluminescence spectra can be represented as quasi-continuous trap distributions. We use the procedure described by Brylew et al.² to determine the trap parameters, assuming an arbitrary value of the frequency factor for distribution at 10^{11} s^{-1} . The fit procedures are shown in Figure S5 and the fit parameters are tabulated in Table S5.

Supplementary Table S5. Parameters of the thermoluminescence peak fitting, where T_{max} is temperature where the maximum of the peak occurs, E is the trap depth, n_0 is the trap concentration and s is the frequency factor.²

Sample	T_{max} (K)	E (meV)	n_0 (a.u.)	s (s^{-1})
Li-doped $\text{PEA}_2\text{PbBr}_4$	45	10.8	6.95×10^5	0.101
	78	41.7	3.17×10^5	4.54
	114	124	1.94×10^5	4.11×10^3
Li-doped BA_2PbBr_4	29	40.5	2.08×10^3	5.28×10^5
	91	107	5.47×10^3	2.12×10^5
	113	155	2.01×10^3	2.33×10^5



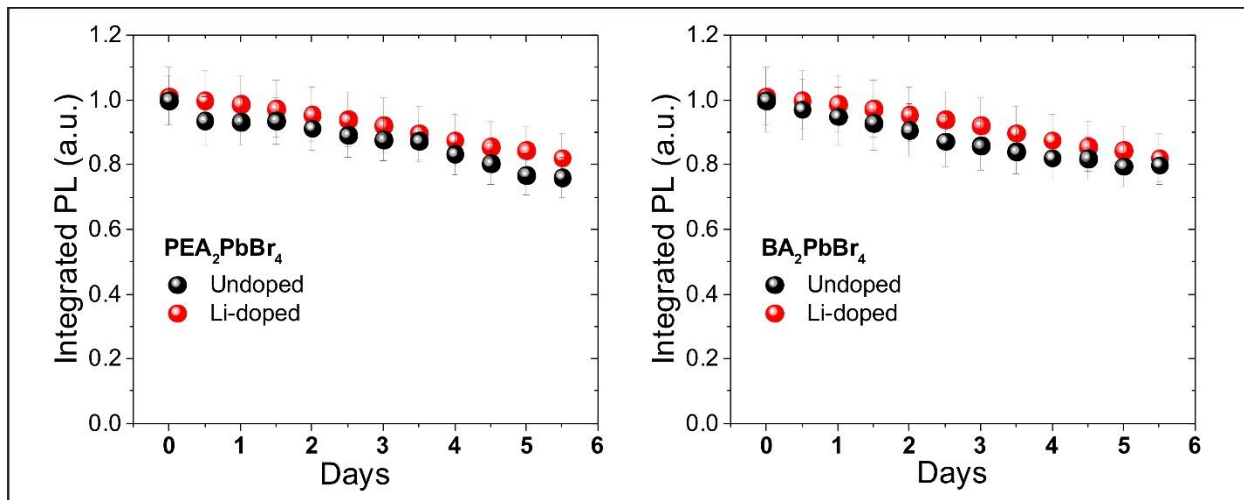
Supplementary Figure S6. Current-voltage curves for undoped and Li-doped PEA₂PbBr₄ (left) and BA₂PbBr₄ (right) measured in dark and under UV light (340 nm, 60 mW). The response to the light, particularly for undoped perovskites, is minimal and the curves show overlap with the dark ones.



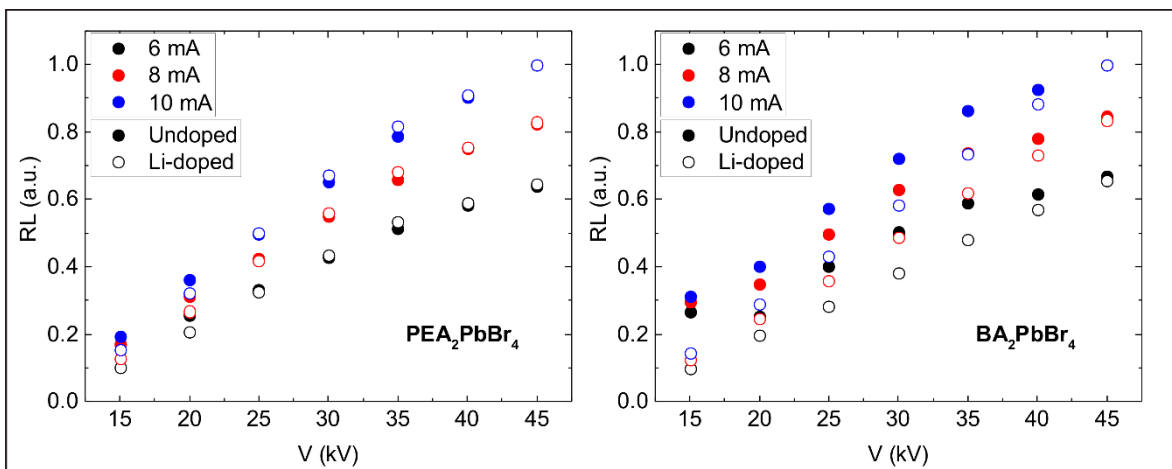
Supplementary Figure S7. (a) Fitting of a decay curve of BA_2PbBr_4 , using a mono-exponential decay function, held at constant X-ray irradiation (source held at 15 kV and 8 mA). (b) Normalized decay time, τ_d , for the undoped and Li-doped perovskites held at constant X-ray irradiation (at $I=8$ mA). Data collected at room temperature.

Supplementary Table S6. Decay times of the room temperature RL held at constant X-ray irradiation (at $I=8$ mA).

Voltage (kV)	Decay Time (s)			
	$\text{PEA}_2\text{PbBr}_4$ Undoped	$\text{PEA}_2\text{PbBr}_4$ Li-doped	BA_2PbBr_4 Undoped	BA_2PbBr_4 Li-doped
15	422	1,315	709	1,579
30	976	10,921	1,458	10,658
45	1,114	26,450	2,334	20,920



Supplementary Figure S8. Photoluminescence intensity vs. time of undoped and Li-doped $\text{PEA}_2\text{PbBr}_4$ (left) and BA_2PbBr_4 (right) while exposed to environmental conditions (standard atmosphere, 65 % humidity).



Supplementary Figure S9. Peak values of the normalized RL of the undoped and Li-doped perovskites at room temperature at different voltage and current applies to the X-ray source.

Supplementary Table S7. Normalized light yield for the undoped and Li-doped perovskites at different gamma-ray excitation energies. The values were normalized for the respective undoped samples at an energy of 662 keV.

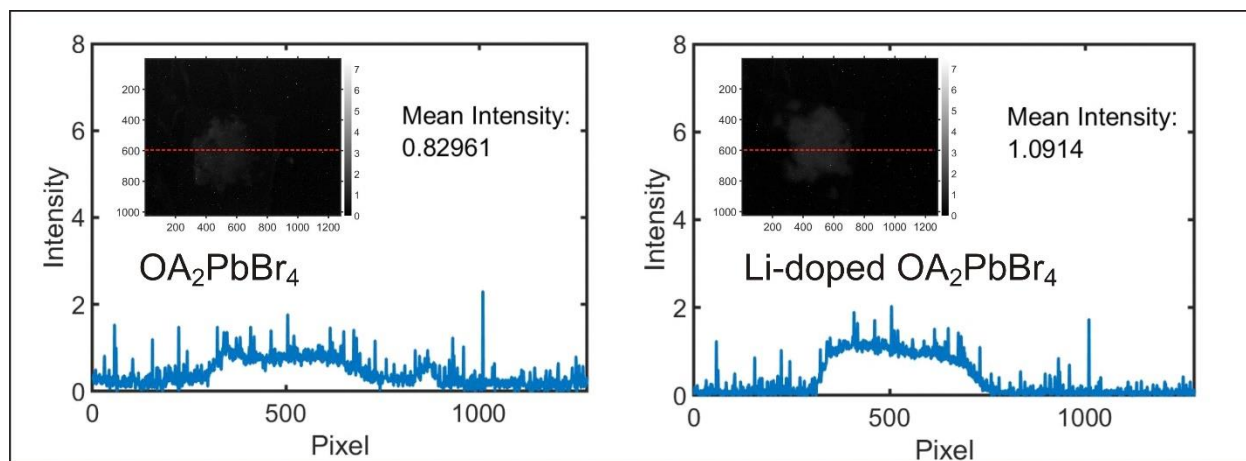
Energy (keV)	Light Yield (normalized to the undoped perovskite at 662 keV)			
	Undoped PEA ₂ PbBr ₄	Li-doped PEA ₂ PbBr ₄	Undoped BA ₂ PbBr ₄	Li-doped BA ₂ PbBr ₄
59.5	0.75 ± 0.10	1.59 ± 0.07	1.10 ± 0.07	0.89 ± 0.07
511	1.02 ± 0.14	1.74 ± 0.08	1.06 ± 0.07	0.71 ± 0.07
662	1.00 ± 0.18	1.78 ± 0.07	1.00 ± 0.06	0.80 ± 0.07

Supplementary Table S8. Energy resolution of the undoped and Li-doped perovskites at different gamma-ray excitation energies.

	Energy Resolution (%)			
Energy (keV)	Undoped PEA₂PbBr₄	Li-doped PEA₂PbBr₄	Undoped BA₂PbBr₄	Li-doped BA₂PbBr₄
59.5	43.1 ± 2.1	32.6 ± 1.3	41.9 ± 2.6	41.0 ± 2.1
511	16.8 ± 1.6	15.6 ± 1.9	19.3 ± 2.1	23.4 ± 1.6
662	11.2 ± 1.7	9.5 ± 2.0	13.0 ± 1.5	10.9 ± 1.7

Supplementary Table S9. Fitting parameters for the scintillation decay of the investigated perovskites under gamma-ray excitation ($E= 662$ keV) fitted with a multiple exponential decay, where τ_i is the decay time, C_i is the contribution of the decay time and $\bar{\tau}$ is the mean time of the decay.

Sample	Decay parameters τ_i (ns) / C_i (%)	Average Gamma-ray Excited Decay Time τ_γ (ns)	Average RL Decay Time³ $\bar{\tau}_{RL}$ (ns)
Undoped PEA ₂ PbBr ₄	13.4 / 94.9 73.7 / 5.1	16.5	12.3
Li-doped PEA ₂ PbBr ₄	11.2 / 98.1 100 / 1.9	12.9	n/a
Undoped BA ₂ PbBr ₄	4.73 / 87.1 20.0 / 11.3 104 / 1.5	8.0	5.3
Li-doped BA ₂ PbBr ₄	4.80 / 87.6 20.8 / 10.9 108 / 1.4	8.0	n/a



Supplementary Figure S10. The X-ray luminescence intensity of undoped (left) and Li-doped (right) octylammonium lead bromide. Insets show the raw imaging data, and the red dotted line shows where the data points were taken for the intensity profile.

References

1. Shibata, H., Negative Thermal Quenching Curves in Photoluminescence of Solids. *Jpn. J. Appl. Phys* **1998**, 37 (Part 1, No. 2), 550-553.
2. Brylew, K.; Drozdowski, W.; Wojtowicz, A. J.; Kamada, K.; Yoshikawa, A., Studies of low temperature thermoluminescence of GAGG:Ce and LuAG:Pr scintillator crystals using the T_{max}-T_{stop} method. *J. Lumin.* **2014**, 154, 452-457.
3. Xie, A.; Maddalena, F.; Witkowski, M. E.; Makowski, M.; Mahler, B.; Drozdowski, W.; Springham, S. V.; Coquet, P.; Dujardin, C.; Birowosuto, M. D.; Dang, C., Library of Two-Dimensional Hybrid Lead Halide Perovskite Scintillator Crystals. *Chem. Mater.* **2020**, 32 (19), 8530-8539.